

## INVESTIGATION IN THE MECHANICAL BEHAVIOR OF LOW-VELOCITY IMPACTED CFRP PLATES UNDER DIFFERENT BOUNDARY CONDITIONS

S. Arslan<sup>1</sup>, M.Z. Sadeghi<sup>1</sup>, A. Dafnis<sup>1</sup> and K.-U. Schroeder<sup>1</sup>

<sup>1</sup> Institute of Structural Mechanics and Lightweight Design (SLA) RWTH Aachen University  
Wuellnerstr. 7, 52062 Aachen, Germany  
sueleyman.arslan@rwth-aachen.de, zamaan.sadeghi@sla.rwth-aachen.de, dafnis@sla.rwth-aachen.de,  
kai-uwe.schroeder@sla.rwth-aachen.de

**Keywords:** Low Velocity Impact, Carbon Fiber Reinforced Polymer (CFRP), Delamination, Finite Element Method, Boundary Condition (BC), NDT techniques

**Abstract.** *The mechanical behavior of Carbon Fiber Reinforced Polymer (CFRP) plates with different boundary conditions (BC) under low velocity impact is investigated experimentally using a drop tower test. To achieve different strain rates, the drop tower's impactor is released from different heights. Two NDT techniques namely the Infrared Lock-In Thermography (IR) and the Ultrasonic Test Method (UT) are applied to detect the damage, i.e. invisible delamination patterns in the plates, which are induced by a metallic hemispherical impactor.*

*A numerical model is developed to simulate the impact tests using the commercial software LS-Dyna. To validate the developed numerical model experimentally, two BCs namely fixed and quasi-freely supported are designed. However, numerical modeling of realistic fixed BCs (by using steel frames with screws) is difficult to be realized (due to undesirable local clumping effects, which induce initial inhomogeneous stress distributions, etc.) and also designing such a test-rig is a time consuming and expensive process. Therefore, another experimental test-rig is designed as an alternative to overcome such problems in the validation process of the developed numerical model. In the proposed test-rig, plates are directly supported on a specific elastomeric pad to represent a quasi-free BC.*

*A good agreement between the experimentally detected damage and numerical results is observed. The proposed quasi-free BC shows a high potential to be an alternative for the fixed BCs in the validation process especially for parametric studies. Meanwhile, comparison between two different BCs designed in this work leads to the following results: Using quasi-free BC results to the reduction in the impact load and consequently smaller shear stress distribution and bending moment comparing to plates with fixed supports. Such an effect leads to reduction in the damage size and slight change in the damage pattern in freely supported plates.*

## 1 INTRODUCTION

Composite panels are attracting increasing attention in a great variety of transportation industries (such as aerospace, marine, automotive, etc.) due to their high strength/weight ratio. Such structures might experience the impact event (low or high velocity) by external objects while they are in service. The impact event induces different damages in the composite panels such as matrix cracks, fiber breakage and more importantly delamination (inter-laminar cracking), which are called Barely Visible Impact Damage (BVID). Such damages can drastically reduce the strength of the laminate. The mechanical behavior of composite structures under impact has been well studied over last decades [1-3].

Some parts of the studies on this research domain are focused on the experimental observations combined with measurement techniques (i.e. Ultrasonic C-scan, X-ray Computed Tomography (CT), etc.) in order to provide a better understanding of the damage mechanism happening during the impact event [4-10]

Alternatively, since testing composites experimentally under impact loadings is an expensive and troublesome task, there have been many efforts within last few years in investigating the damage behavior of such structures numerically and analytically. These works mainly provide numerical frameworks for inter-laminar and intra-laminar caused due to the impact event using stress/strain based criteria (for the onset of the damage) and fracture mechanics (for the propagation of the damage) [11-13] or modeling discrete damage by using interface cohesive zone models (CZM) [14-16].

In spite of the efforts carried out to model the damage mechanism numerically, however, experimental testing should be considered to validate developed numerical frameworks. In this contribution, as a part of validation process of a developed numerical model, the effect of BCs on the damage response of CFRP plates under low velocity impact has been investigated. Designing realistic fixed BCs (using steel frames with screws) is an expensive and time consuming process especially for parametric studies. Meanwhile, considering different effects existing in the fixed BC, such as undesirable local effects which leads to initial inhomogeneous stress distributions in the edges of the laminate, in the numerical model is very difficult. Therefore, another alternative test-rig (quasi free BC using elastomeric pads) is proposed for the validation of the developed numerical model in order to overcome the abovementioned problems for the fixed BCs.

A good agreement between the experimental and numerical results is observed. Considering the effort needed for the designing the quasi-free BC – which is much less than the fixed BC, quasi-free BCs have a good alternative for validation process. Meanwhile, the effect of the different BCs under mechanical behavior under low velocity impact can be summarized as follow: The quasi-freely supported plates can dramatically decrease the impact load leading to smaller bending moment as well as shear stress distribution and consequently reduction in the damage size delamination comparing to the fixed BCs. It is also observed that BC can affect the damage pattern slightly especially in the lower impact velocities.

## 2 EXPERIMENTAL SETUP

The low velocity impact event is created by using a drop tower test. The drop tower test setup was designed and calibrated already in SLA, RWTH Aachen University and was validated in previous works [17]. The setup has the capability to release the impactor (with the weight range of 0.7 to 2.4 kg) up to 5 meters height on the specimens with maximum dimension of 1400x600x70 mm<sup>3</sup> (Figure 1).

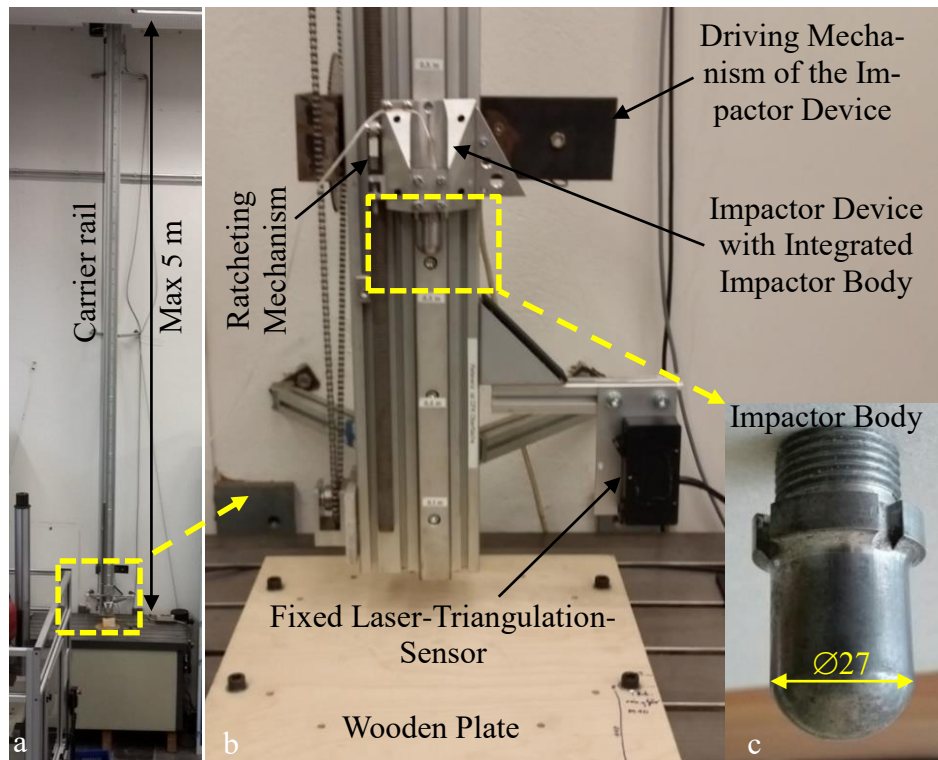


Figure 1: Experimental setup: (a) drop tower, (b) impactor support setup, (c) impactor body

In this work, a cylindrical steel impactor body (Figure 1 (c)) is integrated in an aluminum driving mechanism being able to be released from different heights on the composite panel to achieve strain rates from 480 to 1400 1/s, with respect to the thickness of the plate. The impactor body with the weight of 154 g and diameter of 27 mm has a half-hemispherical head. During the impact event, acceleration and vertical distance time histories are recorded using an accelerometer integrated in the impactor body and a laser-triangulation displacement sensor fixed to the carrier rail. The impactor driving device can be moved electrically to the desired height by using a cable. The corresponding heights are controlled by a distance sensor. To avoid a repeated impact on the plate due to the elastic rebound of the impactor device, a ratcheting mechanism is used (Table 1).

Name of the Component	Commercial Name	Capability
Piezoelectric Accelerometer	ICP Type M350A04	5,000g
Laser-Triangulation Displacement Sensor	Micro-Epsilon Type optoNCDT LD 1605-50	Max. range = $\pm 25$ mm Voltage range = $\pm 10$ V
Cable Pull with Trip Wire Distance Sensor	Micro-Epsilon Type WDS-5000-P501-S-U	Max. 5 m

Table 1: Measurement system used in the drop tower setup

The properties of the plate are shown in Table 2.

Material	Dimension [mm <sup>3</sup> ]	Number of layers	Stacking sequence
HTA/6376	250x250x6.24	48	$[(90/45_2/-45_2/90/0_2)s(0/45/-45/0)_2]_s$

Table 2: Properties of the plate

Two different BCs, fixed and quasi-free, are designed to support the impacted plate in the experimental setup, 5 plates for quasi-free and 5 fixed BC.

## 2.1 Fixed BC

In order to create a fixed BC for the plates, a specific setup is designed. The plate is clamped between two rectangular steel frames (steel-S235JR) having the same size of the composite panels. In order to ensure constant pressure distribution over the pre-stressed panels' area, 32xM8 screws with washers are well distributed around the steel frames (Figure 2).

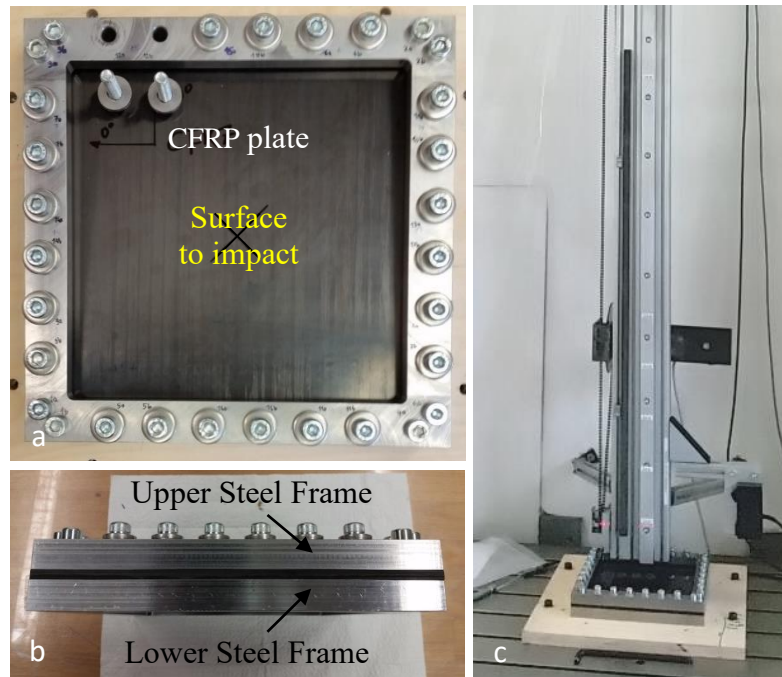


Figure 2: Preparation of the fixed BC: (a) clamping the laminate between two steel frames, (b) side view, (c) attaching the clamped laminate to the wooden part of the drop tower

This arrangement allows acceptable comparison with the numerical model developed for fixed BC. To achieve the constant pressure distribution over the pre-stressed area of the laminate, 70% of the allowable torsional moment for the M8 screws is applied for any screws in a gradual increasing manner. Once the laminate is clamped between the steel frames, the whole frame is bonded to a wooden plate by using 8xM6 screws. The wooden plate attached to the drop tower is used as an interface in order to damp wave transmissions initiated during the impact event.

## 2.2 Quasi-free BC

Quasi-free BC on the plates is achieved by the use of the silicon elastomer named Protectelast®. The behavior of Protectelast under different strain rates was experimentally investigated in previous study [18]. Having had a high capability of elasticity range, 80 % in compression and 640 % in tension, such elastomers can be used as alternative supporting material for representing a quasi-free condition. Using such a material in the BC designed for the plates leads to less constraints in the plate edges and consequently reduction in the stress and strain fields in the laminate edges in comparison to fixed BC. To this end, two rectangular

aluminum frames with the dimension  $305 \times 305 \times 5 \text{ mm}^3$  are manufactured to carry the elastomer pads with thickness of 20 mm (Figure 3).

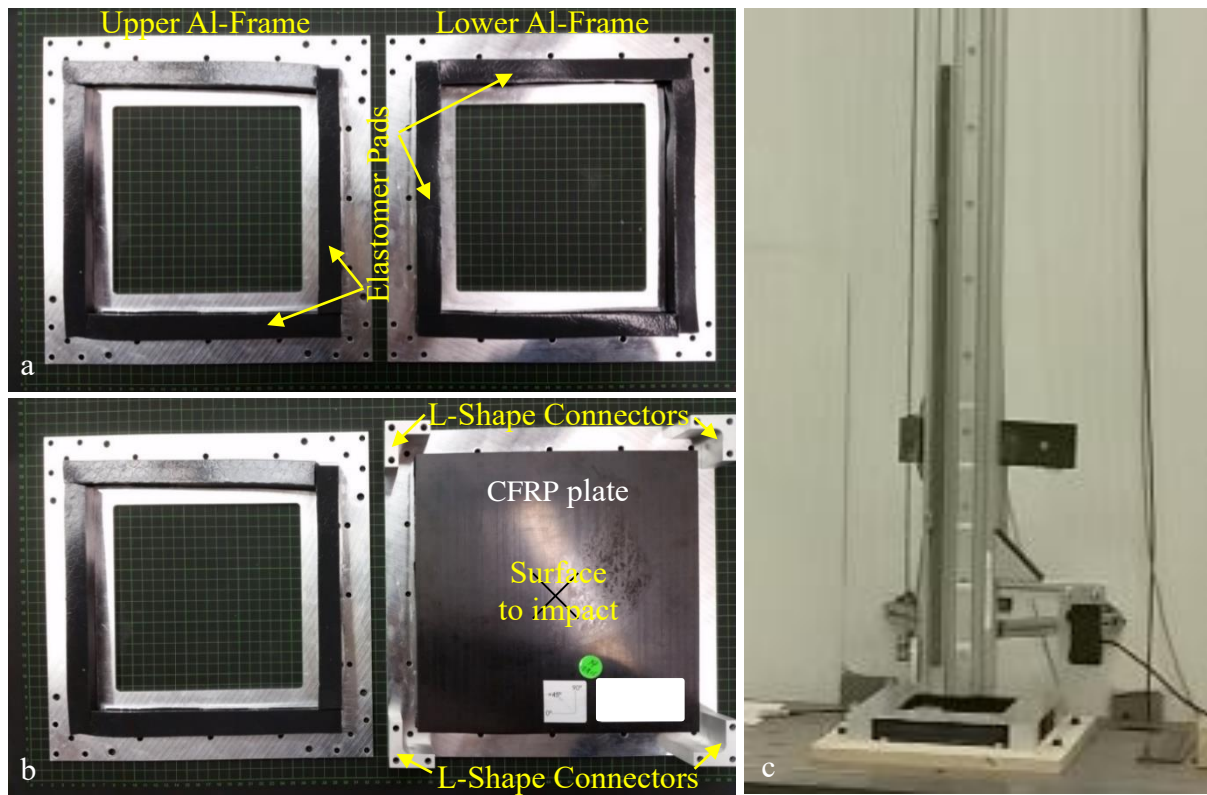


Figure 3: Preparation of the quasi-free BC: (a) inserting elastomers in the aluminum frames, (b) putting the plate on the lower elastomer pads, (c) attaching the clamped laminate to the wooden part of the drop tower

The surface of the aluminum frames are nicely milled to make sure that elastomer pads can be fit inside of the frames. After putting the laminate on the elastomer pad of lower aluminum frame, the upper aluminum frame is assembled on the lower one by using four aluminum L-shape connectors to keep a constant distance between two frames. This distance allows the laminate moves freely between the elastomer pads during the impact event. The final assembly is attached to the wooden plate by using 8xM6 screws.

### 3 FINITE ELEMENT MODEL

The numerical model in this work is developed by using LS-Dyna software. The FE model includes the modeling part for the impactor body, the plate and two BCs applied in the experiments.

#### 3.1 Impactor

The steel impactor body (0.154 kg) and its aluminum impactor device (0.537 kg) are modeled as half-hemispherical solid body with steel material property. However, the weight of the aluminum is considered in the density of the impactor body model. The mesh size at the front side of the impactor, which is in contact with the plate, is about 1.6 mm. The desired velocity is applied to whole impactor body. For the impact event, a node-to-surface contact is used between the impactor and first sub-laminate (explained later). Due to the hemispheric shape of

the impactor, the impactor is selected as the slave and the sub-laminates of the plate as the master.

### 3.2 CFRP plate

The plate is modeled as shell elements using material-enhanced-composite-damage (MAT\_54) as material card in LS-Dyna. This material card gives the possibility to consider the reduction of compressive and tensile strength of the fiber and matrix after intra-laminar failure. Meanwhile, this material card provides the softening reduction factor for material strength in crash front elements. MAT\_54 uses Chang-Chang failure criteria [19]. Material properties used for the plate are listed in Table 3.

Description	Values	Unit
Density	1620	kg/m <sup>3</sup>
Longitudinal Young's Modulus	145	GPa
Transverse Young's Modulus	10.3	GPa
Through-Thickness Young's Modulus	12.1	GPa
Major Poisson's Ratio	0.301	--
Major Transverse Poisson's Ratio	0.5	--
In-Plane Shear Modulus	5.3	GPa
Transverse Shear Modulus	5.275	GPa
Through-Thickness Shear Modulus.	3.95	GPa
Longitudinal Compressive Strength	1600	MPa
Longitudinal Tensile Strength	2250	MPa
Transverse Compressive Strength	290	MPa
Transverse Tensile Strength	64	MPa
In-Plane Shear Strength	98	MPa

Table 3: Material properties for HTA/6376 [22], [23]

#### *Modeling of the Inter-laminar Behavior*

As for the modeling of the delamination pattern induced by the impact event, interface layer based on CZM is used. Interface CZM layers are widely being used by researchers due to many advantages they offer in comparison with other damage modeling techniques [20]. For instance, they are able to predict both the onset and propagation of the damage and they are easy to be implemented in most of simulation software. Since modeling the entire thickness of the CFRP plate with interface layers is quite time consuming (in this case 47 interface layers should be implemented), a special approach is used to model the delamination behavior of this plate. It was previously observed that under impact event, likelihood of delamination is higher between two plies with different fiber orientation [17]. Based on this approach and in order to save the analysis time, we only consider the likelihood of the delamination happening during the impact event only in the layers with the highest differences in their fiber orientations (in this case 90 degree). In this way, for the plate discussed in this work including 48 plies, 14 interface CZM layers have been proposed (Figure 4).

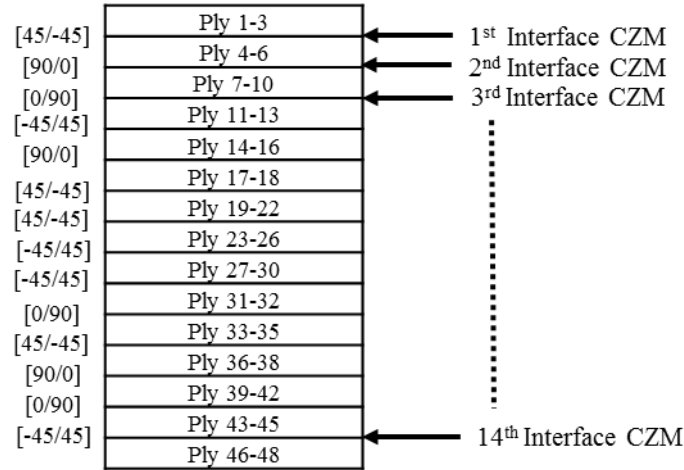


Figure 4: Arrangement of interface CZM layers for the plate

Two numerical methods are available for modeling the interface CZM: the cohesive-zone-element- and the tiebreak-contact-method. In this work tiebreak-contact-method is implemented for modeling the inter-laminar damage, since the cohesive-zone-element-method is too time consuming and therefore unsuitable. Tiebreak option 11 is chosen since it allows using coarser mesh. This contact uses B-K criteria for damage propagation (equation 1). For damage initiation, quadratic nominal stress criterion is applied (equation 2).

$$G_{IC} + (G_{IIC} - G_{IC}) \left( \frac{G_{II}}{G_I + G_{II}} \right)^\mu = G_C \quad (1)$$

$$\left( \frac{\langle \sigma_n \rangle}{N_{max}} \right)^2 + \left( \frac{\langle \sigma_s \rangle}{S_{max}} \right)^2 + \left( \frac{\langle \sigma_t \rangle}{T_{max}} \right)^2 = 1 \quad (2)$$

The mechanical properties for the onset and propagation of the damage for the interface CZM layers are shown in Table 4.

Description	Symbol	Values	Unit
Strain Energy Release Rate for Mode I	$G_{IC}$	260	J/m <sup>2</sup>
Strain Energy Release Rate for Mode II	$G_{IIC}$	1002	J/m <sup>2</sup>
Normal Failure Stress/Peak for Mode I	T	30	MPa
Shear Failure Stress/Peak for Mode II	S	60	MPa
B.K parameter	$\mu$	1.2	--

Table 4: Required parameters for the interface cohesive zone behavior of HTA/6376 [22], [23]

Two different quadratic mesh sizes are considered for the plate. A circular hotspot area with a finer mesh (1.25 mm) is designed with 1.5 time of the biggest delamination area diameter induced by the highest velocity. Coarser mesh is considered outside of this area (2.5 mm). The plate consists of 13,792 elements per sub-laminate (total of 206,880 elements for the whole plate). Since the minimum number of elements needed for CZM should be three elements to capture the process zone happening in the damage propagation [21], a special scaling factor is used to calculate the peak tractions (mode I and II) for coarser mesh sizes.



More explanation about the element sizes and the corresponding scaling factors was provided in a previous work [18].

### 3.3 Boundary Condition (BC)

The numerical model for both BCs is developed with the same dimensions of the original specimens explained in the section 2.1 and 2.2. For more details, a section cut of the model is shown in Figure 5. In fixed BC, the upper and lower steel frames are modeled with solid elements (mesh size of 2.5 mm). The contact between the upper steel frame and the first sub-laminate as well as the contact between the lower steel frame and the last sub-laminate are both considered tied contact. In this way, the constant pressure caused by screws in the specimens is guaranteed. For quasi-free BC, the aluminum frames are modeled by using shell elements whereas the elastomers are modeled as solid elements (mesh size for both elastomers and aluminum frames is 2.5 mm). The mechanical behavior of the elastomer pads under different strain rates were already investigated in a previous study [18].

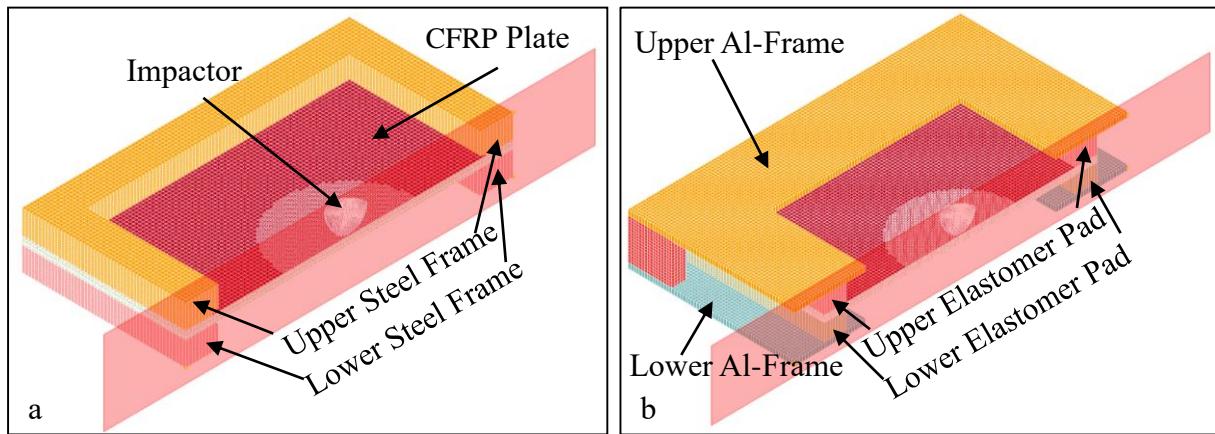


Figure 5: FE Model developed for (a) fixed and (b) quasi-free BC

## 4 RESULTS AND DISCUSSION

As previously mentioned in section 2, 10 sets of experiments in total are carried out in order to investigate the effect of fixed and quasi-free supported plates under different velocities ranging from 3 to 9 m/s. In this section the effect of these two BCs on the impact response of the plates under different impact velocities have been discussed numerically and experimentally.

### *Impact velocity and rebound behavior*

Some experimental results of the impact test are listed in Table 5 and a comparison of velocities is made in Figure 6. The velocities  $V_I$  and  $V_R$  are estimated by measuring the slope of the displacement-time curve of the vertical movement of the impactor (measured by the laser-triangulation sensor). The residence time  $t_R$  is the period between the time at which the impactor hits the plate ( $V_I$ ) and the time at which the impactor separates from the plate ( $V_R$ ).



BC-CFRP <sub>x</sub>	Drop height h [m]	Impact ve- locity V <sub>I</sub> [m/s]	Residence time of the impact event t <sub>R</sub> [ms]	Resultant Deflection d <sub>max</sub> [mm]	Rebound velocity V <sub>R</sub> [m/s]
Quasi-free-CFRP1	1	4.33	4.865	-3.54	1.86
Quasi-free-CFRP2	2	6.22	4.870	-4.92	2.79
Quasi-free-CFRP3	3	7.60	4.745	-6.03	3.12
Quasi-free-CFRP4	4	8.54	4.660	-6.80	3.37
Quasi-free-CFRP5	4.61	8.79	4.645	-6.82	3.44
Fixed-CFRP6	0.5	3.05	<1.755*	<-2.57*	2.50
Fixed-CFRP7	1	4.37	1.755	-2.57	3.71
Fixed-CFRP8	2	6.17	1.795	-3.48	5.18
Fixed-CFRP9	3	7.52	1.900	-4.37	5.90
Fixed-CFRP10	4	8.74	1.890	-5.81	6.61

Table 5: Results for the impact tests

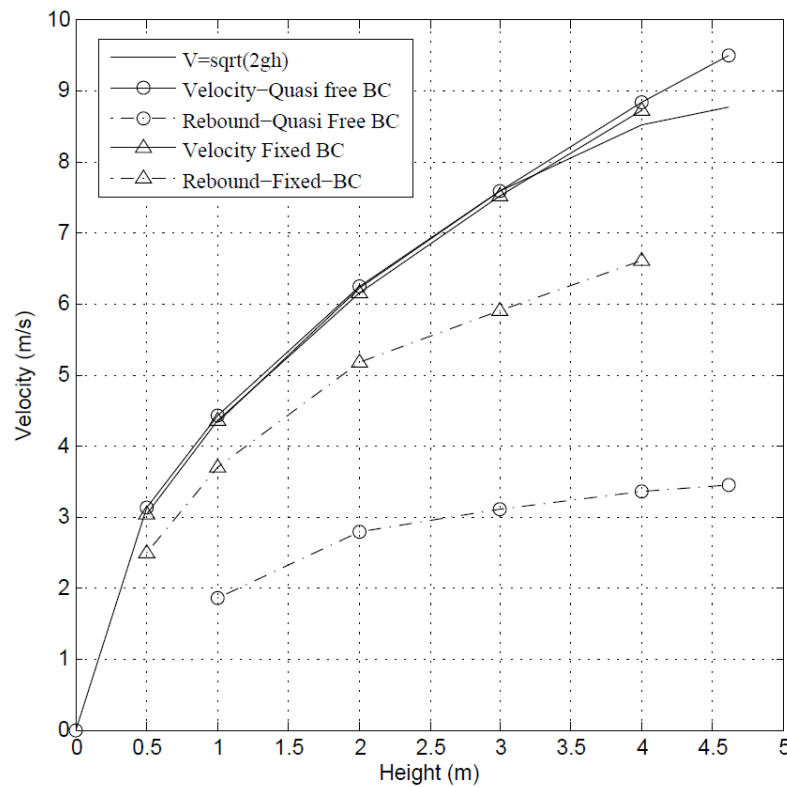


Figure 6: Comparison of the impact and rebound velocities for different BCs

As expected, almost all 10 impact velocities are close to the physical law  $V = \sqrt{2gh}$ , which states that friction effects and other disturbance have a very small influence on the velocity. However, as it is shown in Figure 6 the rebound velocity is highly influenced by the type of the BCs. Existence of elastomer in quasi-free BC leads to reduction in the rebound velocity comparing to corresponding plate with the fix support. This reduction mainly induced by the compression of the elastomer within the impact event.

The residence time  $t_R$  for the fixed BCs is shorter than that of the quasi-free. Meanwhile, the resultant deflection  $d_{max}$  is for the fixed BC smaller than for the quasi-free.

\*Could not be measured exactly

In Figure 7, the resultant deflection  $d_{\max}$  and residence time  $t_R$  for CFRP9 and CFRP3 is shown. Such a response is also observed in the other tests. The fixed BC shows a simple impact-rebound-behavior whereas the quasi-free shows a delayed response with a greater resultant deflection, because of the existing of the elastomer. After reaching the maximum value of -6.03 mm the quasi-free shows two rebounding behaviors.

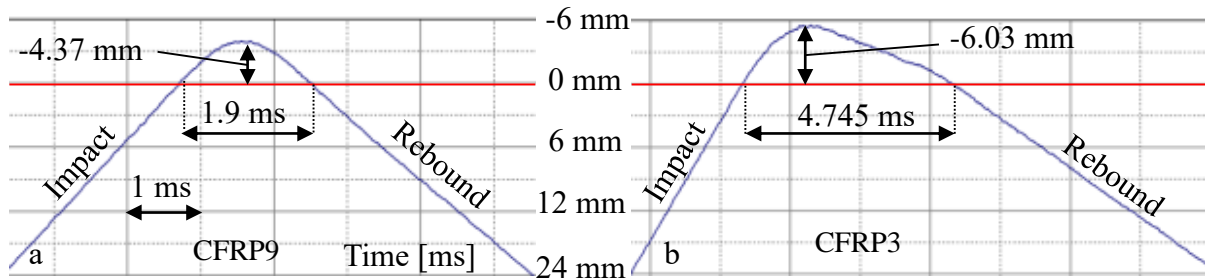


Figure 7: Comparison of the resultant deflection  $d_{\max}$  and residence time of the impact event  $t_R$  for CFRP9 (a) (quasi-free) and CFRP9 (b) (fixed) (red line: CFRP plate surface on the impact side)

### Impact Force

Comparison of the impact force – FE result – between the impactor and the plate for both quasi-free and fixed BC (CFRP5 and 10) is shown in Figure 8.

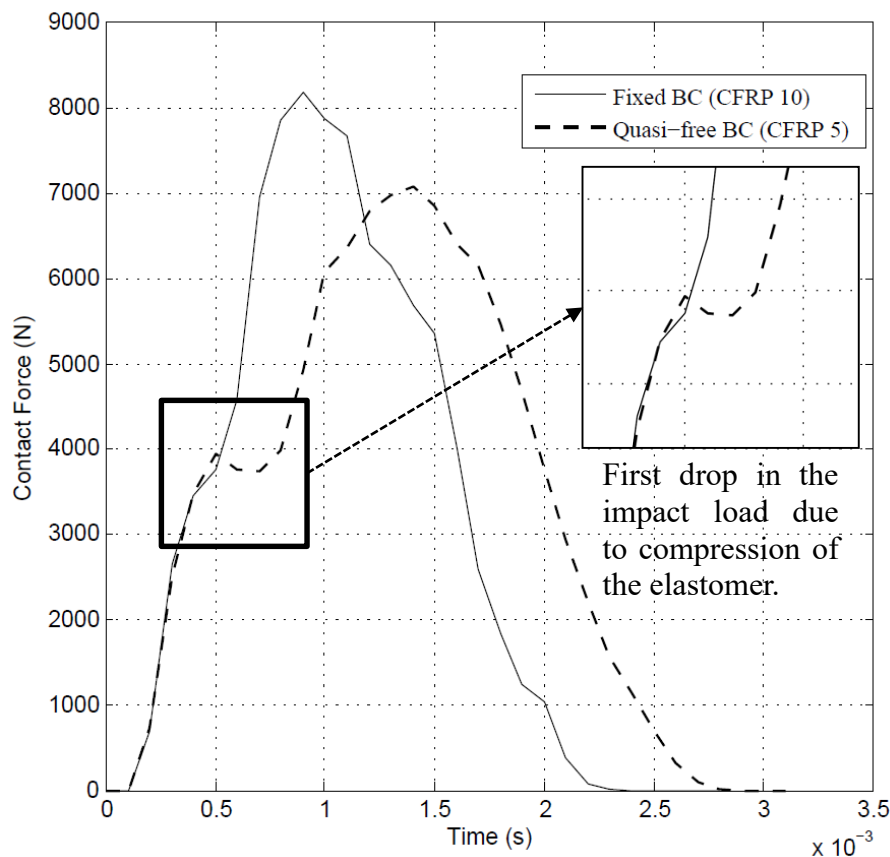


Figure 8: The impact force for fixed and quasi-free BC ( $V_I \approx 9$  m/s)

In quasi-freely supported plates, elastomer undergoes sever compression during the impact event causing a drop in the contact force comparing to the plates supported with fixed BC (the frame is rigid). At the same time at which elastomer causes a drop in the contact force for quasi-free BC, contact load for the plate with fixed support shows a disturbance in the load response, which clearly indicate the effect of fixed BC and introducing more bending moment to the system, which dramatically increases the contact force. At the peak point of the both curves, the maximum delamination area is observed in which the damage area remains constant over time.

### *Damage size*

For experimental observations two measurement techniques namely Ultrasonic and active Lock-in Thermography technique are used in order to determine the damage induced by the impact event in plates. Ultrasonic method is applied on top and through the thickness of the impacted plates to spot the damage area. This technique provides us qualitative and distinctive images of the damaged area but not quantitatively. This technique only provides the concentration of the damage on the first damaged area, which is detected by the device and the damage on the other layers are not shown in the results. Thermography technique provides us top view of the damage accumulation of the impacted plates. This technique is only able to detect damages happening up to around 4 mm from the surface of the plate.

In Figure 9, a comparison for the induced damage between two panels (CFRP5 and 10), which are impacted by the same velocity ( $\cong 9 \text{ m/s}$ ) but different boundary conditions is shown, which includes Ultrasonic, Thermography (phase image) and FE observations.

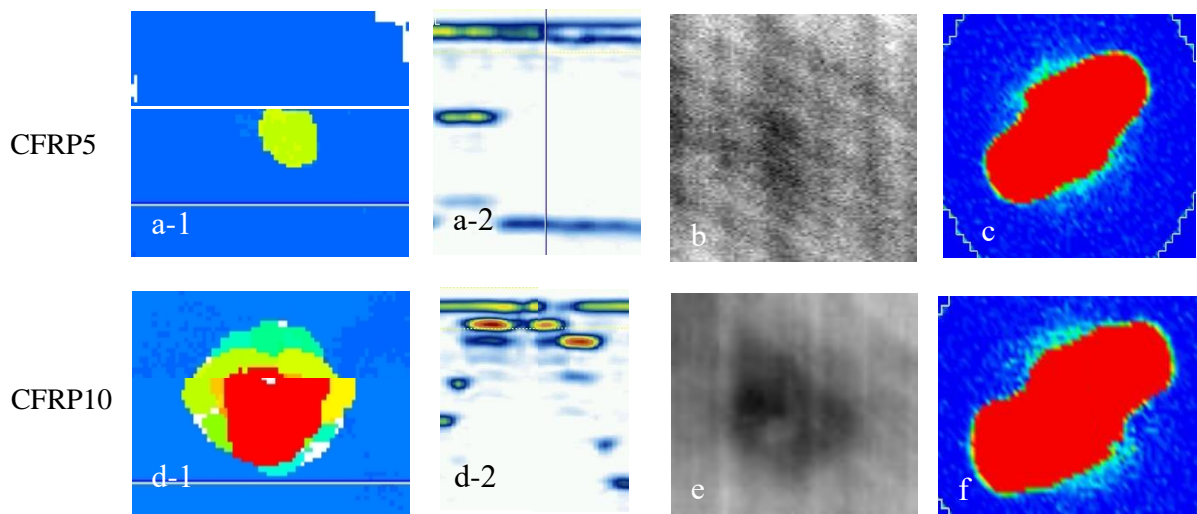


Figure 9: Comparison of the delamination: (a) and (d) ultrasonic, (b) and (e) thermography, (c) and (f) numerical

In Ultrasonic observations shown in Figure 9 the color red (the images on the top view) represents the damages exists on the first interface layer close to the surface of the plates, yellow represents the damages exist in the middle, green represents the damages in the sub laminates close to the bottom of the plates, and blue represent the undamaged area (bottom of the plate).

At the first glance, the comparison between the plates shows that the size of the induced damage by the impactor in fixed BC is bigger than the same panel with quasi-free BC. The same result is observed for other panels too. It can be attributed to the bigger bending moment

(and also shear stress distribution) existing in the panels supported with fixed BC comparing to quasi-freely supported panels leading to bigger damage in the panels.

For the CFRP5 (quasi-freely supported) the biggest induced damage is in the middle, the same result in the FE model in which interface layer number 7 shows the biggest damage area comparing to other interface layers. The damage induced in the middle of the CFRP5 is shown in the through the thickness Ultrasonic image (Figure 9 (a-2)). In the CFRP10, the top view of the Ultrasonic image shows that damage in the middle of the plate is bigger (yellow color) showing a good agreement with the FE results (7th interface layer). The through thickness Ultrasonic image (Figure 9 (d-2)) shows that the damage is only on the surface since the system is only able to spot the first damaged region (region close to the surface of the plate (red color in (d-1) and the rest of the damaged area – in this view – cannot be spotted. Thermography observations (Figure 9 (b) and (e)) show a good agreement with the other results. Comparison between Figure 9, (b) and (e) clearly shows that the damage due to the impactor under fixed BC is bigger than quasi-free BC.

Distribution of the shear stress for both BCs is shown in Figure 10 showing greater stress contour in the fixed BC especially at the edges.

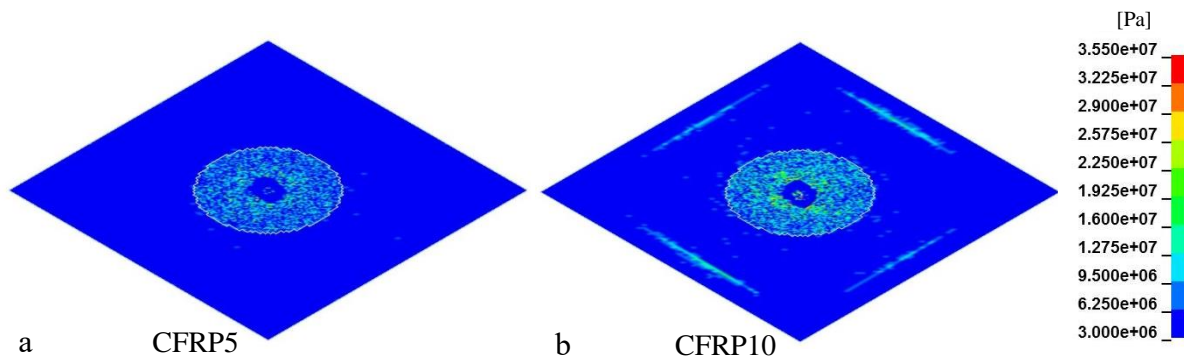
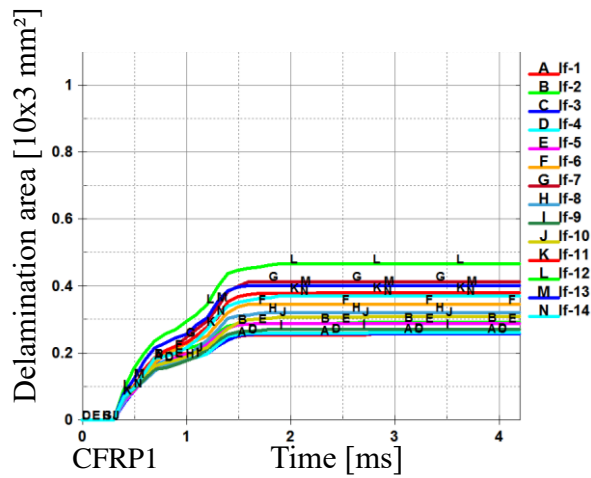


Figure 10: Shear distribution of the first interface layer: (a) quasi-free, (b) fixed BC

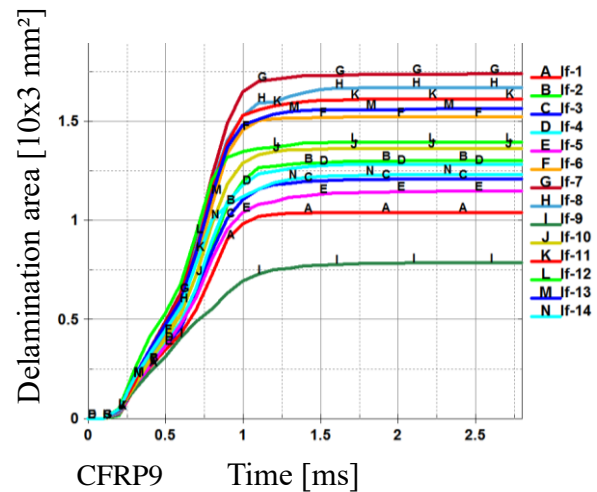
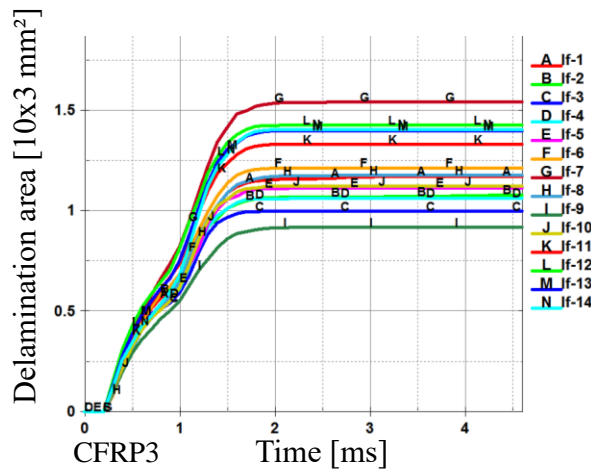
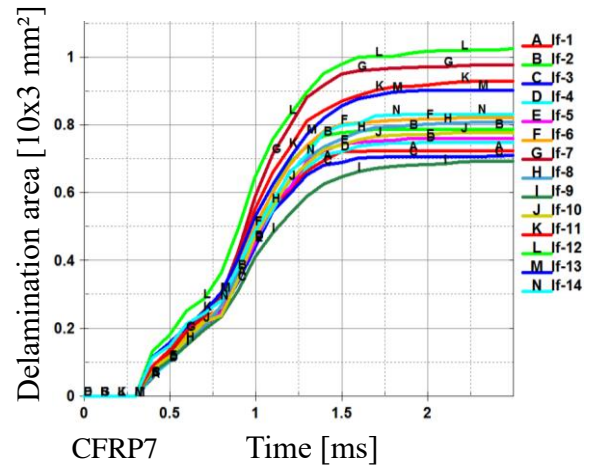
The evolution of the damage area over time for the composite panel for different BCs under different impact velocity is shown in Figure 11.

It can be clearly seen that for a certain velocity, the damage area is always bigger for the fixed supported panels. In both boundary conditions, a frustum-conical damage pattern is observed. For the plates impacted under fixed boundary condition this pattern is larger (in both upper and lower area of the frustum). However, when it comes to the quasi-free BC, the differences between the upper base and lower base of the frustum-conical damage pattern is becoming smaller (especially under lower velocities (CFRP1)) and damage pattern is more circular like. As it was previously discussed, Lock-in Thermography camera works based on the change of the frequency. In this method, the values of the frequency should be changed till a visible damage accumulation is achieved. However, this method is only able to detect the damage exists up to around 4 mm thickness (from the surface of the plate). Since in this work, all the plates have the same thickness of 6.24 mm, detecting the damage accumulation existing in the lower layers (bigger than 4 mm depth) is very difficult.

## Quasi-free BC



## Fixed BC

Figure 11: Delamination area from numerical results (A Jf-1=1<sup>st</sup> and N Jf-14=14<sup>th</sup> interface CZM layer)

A good example is the comparison between CFRP9 and CFRP3, same panel impacted under velocity of about 7.6 m/s but with different BCs. Due to the constrained applied in CFRP9, the induced impact damage is bigger comparing to the other plate. Figure 12 shows that the suitable image of the damage accumulation can be simply detected in such a panel by changing the lock-in frequency.

In contrast, CFRP3 – which is impacted under quasi-free BC – experiences smaller damages in the layers. In Figure 13, the growth of the area of the delamination versus elapsed time is shown. The induced damage in most of the interface layers is very small and there is only in the interface layer number 12 in which the damage area is slightly bigger. However, it is difficult in Lock-in Thermography method to detect such a damage, which is located in a depth of about 5 mm from the surface of the plate. Hence the reason, Lock-in Thermography is not able to spot a decent damage accumulation in the plate. Figure 14 visibly shows that even changing the frequencies does not detect a good damage accumulation.



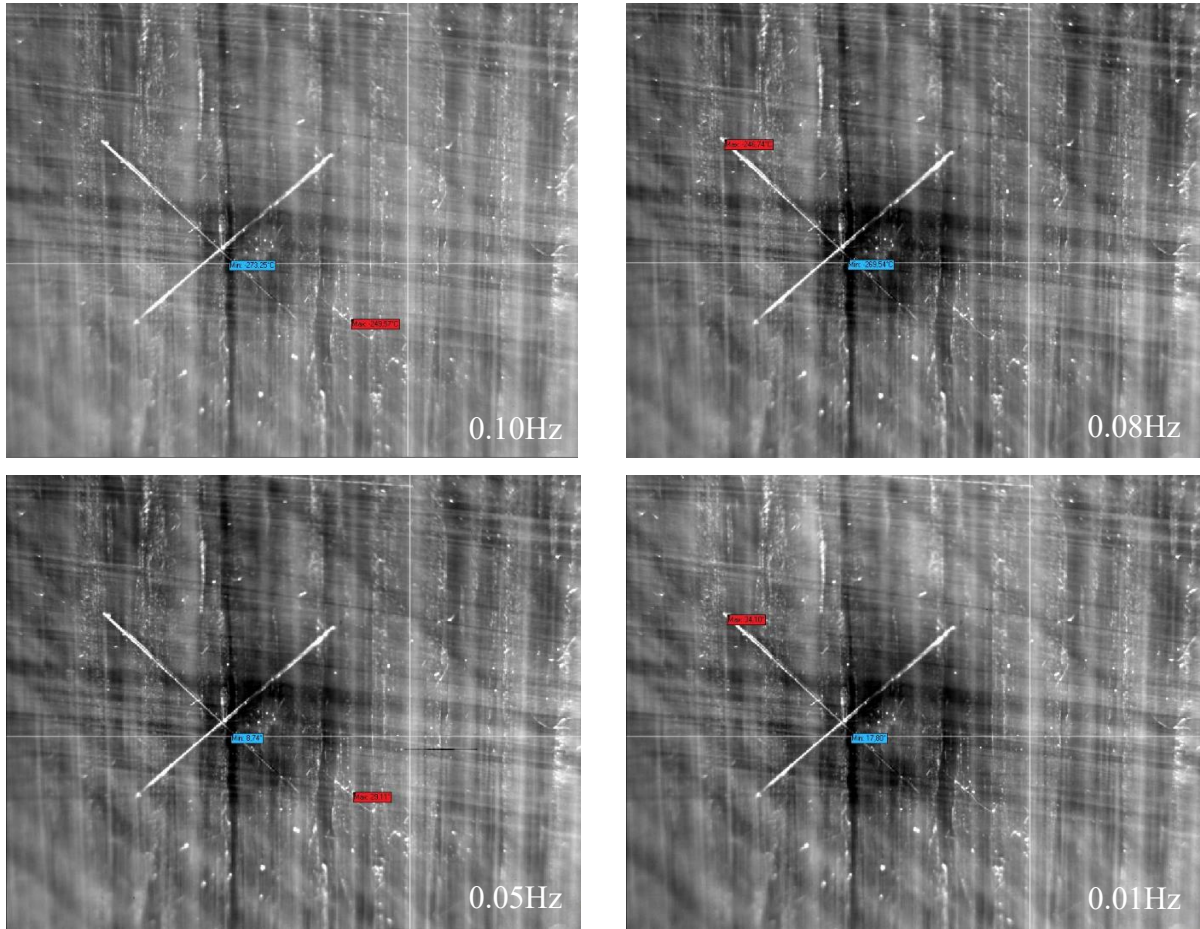


Figure 12: Damage measurement using Lock-in Thermography camera with different lock-in frequencies-CFRP9

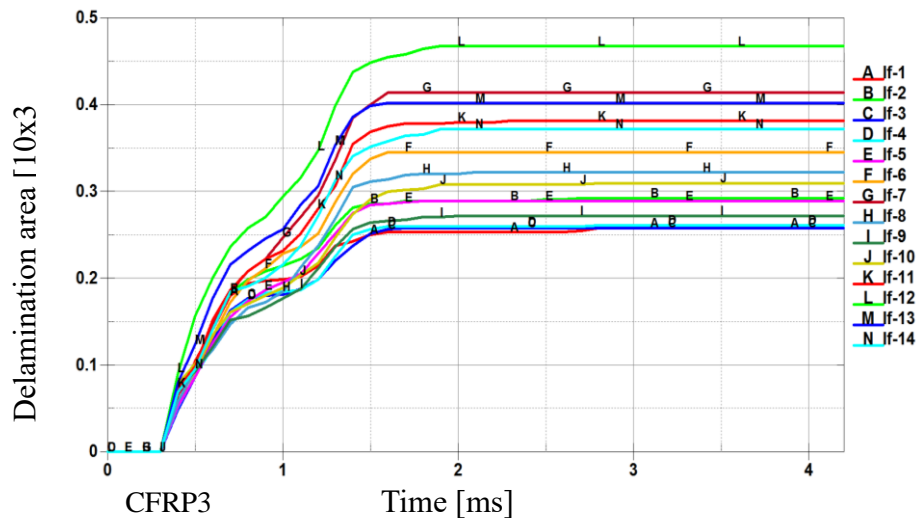


Figure 13: Delamination area of numerical results (A lf-1=1<sup>st</sup> and N lf-14=14<sup>th</sup> interface CZM layer)



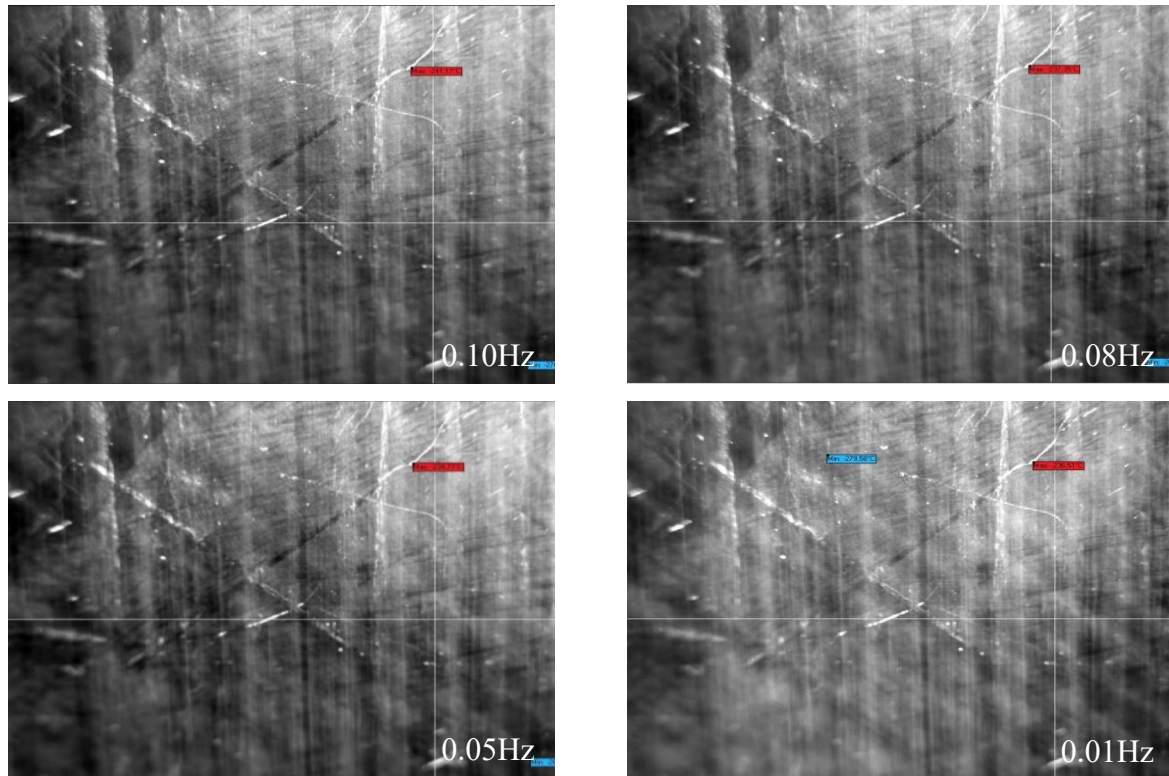


Figure 14: Damage measurement using Lock-in Thermography camera with different lock-in frequencies-CFRP3

## 5 CONCLUSIONS

The mechanical behavior of Carbon Fiber Reinforced Polymer (CFRP) plates (made of HTA/6376 with the dimension of 250x250x6.24 mm<sup>3</sup>) and with different boundary conditions (BC) under low velocity impact is investigated experimentally using a drop tower test. Two NDT techniques namely the Infrared Lock-In Thermography (IR) and the Ultra-sonic Test Method (UT) are applied to detect the damage induced by a metallic hemispherical impactor.

A numerical model is developed to simulate the impact tests using the commercial software LS-Dyna. In order to validate the developed numerical model experimentally, two boundary conditions namely fixed and quasi-freely supported are designed. A good agreement between the experimental observations using NDT methods and numerical results is achieved. The proposed quasi-free BC shows a high potential to be an alternative for the fixed BCs in the validation process especially for parametric studies. Meanwhile, comparison between two different boundary conditions designed in this work leads to the following results: Using quasi-free BC reduces the impact load and consequently smaller shear stress distribution and bending moment comparing to plates with fixed supports. This leads to reduction in the damage size and slight change in the damage pattern in freely supported plates.

## ACKNOWLEDGEMENT

The authors wish to thank the European Commission Research Directorates financial support in the framework of Clean-Sky project JTI-CS-2011-03-SFWA-02-019. We also would like to give a special thanks to Werkzeugmaschinenlabor (WZL) RWTH Aachen who provided us with the Ultrasonic images.

## REFERENCES

- [1] M.O.W. Richardson, M.J. Wisheart, Review of low-velocity impact properties of composite materials, *Composites Part A: Applied Science and Manufacturing*, Volume 27, Issue 12, 1996, Pages 1123-1131.
- [2] W.J. Cantwell, J. Morton, The impact resistance of composite materials — a review, *Composites*, Volume 22, Issue 5, 1991, Pages 347-362.
- [3] Agrawal, Sandeep, Kalyan Kumar Singh, and P. K. Sarkar. "Impact damage on fibre-reinforced polymer matrix composite—a review." *Journal of Composite Materials* (2013): 0021998312472217.
- [4] M.V. Hosur, C.R.L. Murthy, T.S. Ramamurthy, Anita Shet, Estimation of impact-induced damage in CFRR laminates through ultrasonic imaging, *NDT & E International*, Volume 31, Issue 5, October 1998, Pages 359-374.
- [5] Catherine Potel, Thierry Chotard, Jean-François de Belleval, Malk Benzeggagh, Characterization of composite materials by ultrasonic methods: modelization and application to impact damage, *Composites Part B: Engineering*, Volume 29, Issue 2, 1998, Pages 159-169
- [6] F Aymerich, S Meili, Ultrasonic evaluation of matrix damage in impacted composite laminates, *Composites Part B: Engineering*, Volume 31, Issue 1, January 2000, Pages 1-6.
- [7] B.S. Ben, B.A. Ben, K.A. Vikram, S.H. Yang, Damage identification in composite materials using ultrasonic based Lamb wave method, *Measurement*, Volume 46, Issue 2, February 2013, Pages 904-912, ISSN 0263-2241.
- [8] M. Tehrani, A.Y. Boroujeni, T.B. Hartman, T.P. Haugh, S.W. Case, M.S. Al-Haik, Mechanical characterization and impact damage assessment of a woven carbon fiber reinforced carbon nanotube–epoxy composite, *Composites Science and Technology*, Volume 75, 11 February 2013, Pages 42-48.
- [9] S.A. Grammatikos, E.Z. Kordatos, T.E. Matikas, C. David, A.S. Paipetis, Current injection phase thermography for low-velocity impact damage identification in composite laminates, *Materials & Design*, Volume 55, March 2014, Pages 429-441.
- [10] E. Abisset, F. Daghia, X.C. Sun, M.R. Wisnom, S.R. Hallett, Interaction of inter- and intralaminar damage in scaled quasi-static indentation tests: Part 1 – Experiments, *Composite Structures*, Volume 136, February 2016, Pages 712-726.
- [11] P. Maimí, P.P. Camanho, J.A. Mayugo, C.G. Dávila, A continuum damage model for composite laminates: Part II – Computational implementation and validation, *Mechanics of Materials*, Volume 39, Issue 10, October 2007, Pages 909-919
- [12] M.V. Donadon, L. Iannucci, B.G. Falzon, J.M. Hodgkinson, S.F.M. de Almeida, A progressive failure model for composite laminates subjected to low velocity impact damage, *Computers & Structures*, Volume 86, Issues 11–12, June 2008, Pages 1232-1252
- [13] Y. Shi, T. Swait, C. Soutis, Modelling damage evolution in composite laminates subjected to low velocity impact, *Composite Structures*, Volume 94, Issue 9, September 2012, Pages 2902-2913.
- [14] F. Aymerich, F. Dore, P. Priolo, Prediction of impact-induced delamination in cross-ply composite laminates using cohesive interface elements, *Composites Science and Technology*, Volume 68, Issue 12, September 2008, Pages 2383-2390.
- [15] M.F.S.F de Moura, J.P.M Gonçalves, Modelling the interaction between matrix cracking and delamination in carbon–epoxy laminates under low velocity impact, *Composites Science and Technology*, Volume 64, Issues 7–8, June 2004, Pages 1021-1027.

- [16] Stephen R. Hallett, Wen-Guang Jiang, Bijoy Sri Khan, Michael R. Wisnom, Modelling the interaction between matrix cracks and delamination damage in scaled quasi-isotropic specimens, *Composites Science and Technology*, Volume 68, Issue 1, January 2008, Pages 80-89
- [17] S. Woeste, Impact investigation of dog-bone CFRP specimens, PhD thesis, Institute for lightweight design, RWTH Aachen, 2005.
- [18] S. Arslan, A. Dafnis, K.-U. Schroeder, Simulation of Bird Strikes on CFRP Plates as a Part of a Validation Process, ICEAF IV, Skiathos, Greece, 2015.
- [19] Chang, Fu-Kuo; and Chang, Kuo-Yen: A Progressive Damage Model for *Laminated Composites Containing Stress Concentrations*. *J. Compos. Mater.*, vol. 21, Sept. 1987, pp. 834-855.
- [20] M.R. Wisnom, Modelling discrete failures in composites with interface elements, *Composites Part A: Applied Science and Manufacturing*, Volume 41, Issue 7, July 2010, Pages 795-805.
- [21] Turon, A., Davila, C.G., Camanho, P.P.; “An Engineering Solution for Using Coarse Meshes in the Simulation of Delamination with Cohesive Zone Modeling”, NASA Technical Report NASA/TM-2005-213547. Langley Research Center, Hampton, Virginia, March 2005.
- [22] M. Ericsson, Simulating Bird Strike on Aircraft Composite Wing Leading Edge, Master Thesis, KTH Engineering Sciences, Stockholm, Sweden, 2012
- [23] K.I. Tserpes, A three-dimensional progressive damage model for bolted joints in composite laminates subjected to tensile loading, Blackwell Science Ltd. *Fatigue Fract Engng Mater Struct* 24, 663–675, 2001
- [24] LS-Dyna Aerospace Working Group, Modeling Guidelines Document, 2015
- [25] F. Dolce F, Blast Impact Simulation on Composite Military Armours, Department of Mechanical Engineering, University of BATH, 2009
- [26] LS-Dyna User’s Manual I and II, 2015